DEVELOPMENT OF VERY LOW FREQUENCY SELF-NULLING PROBE FOR INSPECTION OF THICK LAYERED ALUMINUM STRUCTURES

Buzz Wincheski and Min Namkung
NASA Langley Research Center
Hampton, VA 23681

INTRODUCTION

Nondestructive evaluation technologies have recently been challenged to inspect thick, layered, conducting materials for fatigue and corrosion damage. Structures that fall into this class, such as airframe wings, pose significant difficulties for conventional inspection techniques. Reflections of ultrasound at layer boundaries cause serious problems for the application of ultrasonic inspection methods. Conventional eddy-current inspection techniques are also compromised due to the exponential decay of electromagnetic energy with depth into a conductor.

To perform the required inspections, a very low frequency electromagnetic method has been developed. The use of a low frequency induction source increases the depth of penetration of the field into the sample under test. This allows a significant field intensity to reach the required inspection depths. Detection of small changes in the low frequency field caused by deeply buried flaws is, however, a major challenge. As a possible solution to this challenge, the use of a giant magneto-resistive (GMR) field sensor is examined. The GMR device is highly sensitive to the magnetic field intensity, as opposed to the rate of change of the field as is the case with conventional pickup coil devices. The use of the GMR device, combined with appropriate shielding and flux focusing has enabled the detection of fatigue cracks buried up to 1 centimeter in unflawed aluminum alloy plates.

LOW FREQUENCY EDDY CURRENT INSPECTION OF THICK ALUMINUM COMPONENTS

It is well known that steady state eddy current inspections are governed by the skin depth equation [1, 2]. In CGS units the skin depth equation is given by

$$B_z = B_0 \exp(-z/\delta) \tag{1}$$

$$\delta = c \Big/ \sqrt{2\pi\mu\omega\sigma} \tag{2}$$

where B_z is the magnetic field at depth z into the material under test, B_0 is the magnetic

field at the surface, c is the speed of light, μ is the permeability, ω is the angular frequency, σ is the conductivity, and δ is the skin depth. It is clear from Equation (1) and (2) that an eddy current inspection for deeply buried flaws in a conducting material requires a low frequency of operation. In aluminum alloys typically used in airframe construction with μ=1 and σ=1.7 x 10^{17} sec^{-1}, for example, a frequency of 130 Hz is required for the skin depth to reach 1 centimeter into the material under test. At such frequencies pickup coil type sensors lose sensitivity due to Faraday's law of electromagnetic induction which states

$$\varepsilon = -\frac{A}{c}\frac{dB}{dt} \propto \omega \sin \omega t . \qquad (3)$$

The electromotive force, ε, induced around a circuit is proportional to area enclosed, A, times the time rate of change of the magnetic field through the circuit [1]. As the excitation frequency is lowered the induced voltage across the pickup coil is reduced, reducing the effectiveness of the inspection.

A straightforward method to circumvent the difficulties pointed out above is to replace the inductive pickup sensor with a measurement device that measures the magnetic field directly. Several such mechanisms for the detection of low frequency magnetic fields are well known. These include Hall effect sensors, flux gate magnetometers, squid magnetometers, and giant magneto-resistive devices. Each of the techniques is sensitive to the magnetic field level and is therefore well suited for low frequency inspection. The mechanisms do vary quite dramatically in sensitivity, instrumentation requirements, and linearity. Optimization of a low frequency eddy-current inspection tool requires customizing the induction source and its shielding to maximize the sensitivity of the specific field sensor.

GIANT MAGNTO-RESISTANCE

Giant magneto-resistive sensors have several advantages over the competing technologies for applications to low frequency eddy-current testing [3-5]. The devices are small, low cost, highly sensitive, operate at room temperature, and require minimal instrumentation. Commercial GMR sensors are available which are based upon electron scattering in antiferromagnetically coupled multi-layers. In the absence of an applied field, the resistivity of the device is high due to scattering between oppositely polarized electrons. An external field aligns the magnetic moments of the ferromagnetic layers, eliminating this scattering mechanism and thereby reducing the resistivity of the material [5]. It should be noted that this mechanism is sensitive to the magnitude but not the direction of the external field. The resistivity of the material is high in the absence of an external field and decreases with increasing field magnitude as the moments of the ferromagnetic layers align with the external field direction.

In the application of GMR materials as field sensors it is common to incorporate flux concentrators into the sensor as a means to increase the sensitivity of the device. A schematic diagram of the commercially available sensor used in the present work is shown in figure 1 [5]. The design uses four GMR elements connected in a Wheatstone bridge configuration. Two of the four elements are shielded from the external field. In the absence of an external field all four elements will have the same resistance and no voltage will be detected across the center of the bridge. When an external field is present, the resistivity of the two unshielded GMR elements will drop and a positive voltage will be detected across the bridge. The four GMR elements along with the pictured flux

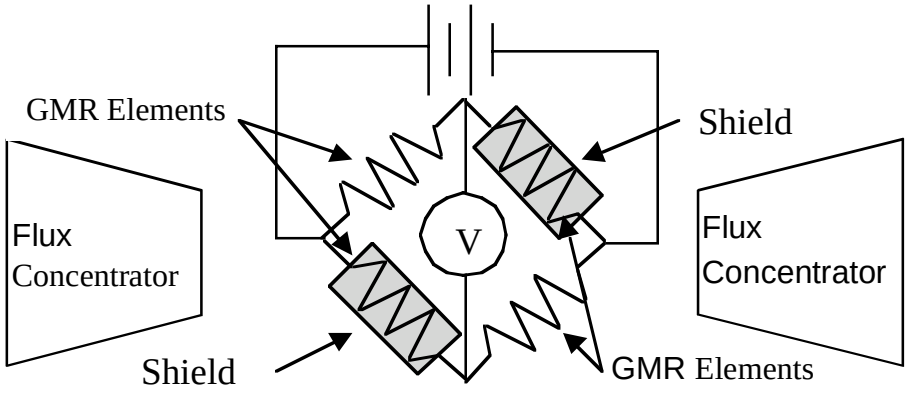

Figure 1. Schematic diagram of commercially available GMR sensor [5].

concentrators are packaged in an eight pin chip.

The design of the Self-Nulling Eddy Current Probe [6] was used as a model for incorporating the GMR sensor into a very low frequency electromagnetic inspection device. The major modification was replacement of the pickup coil of the Self-Nulling Eddy Current Probe with a GMR sensor. Other design considerations of the Self-Nulling Probe, such as using a flux focusing lens wall thickness of at least three skin depths and keeping the height of the pickup sensor less than the half height of the probe, were incorporated into the final design. A schematic diagram of the GMR based Self-Nulling Probe is given in Figure 2.

VERY LOW FREQEUNCY SELF-NULLING PROBE

To interpret the output response of the Very Low Frequency (VLF) Self-Nulling Probe, the sensor was first calibrated in a controlled magnetic field. The sensor was placed in the center of a Helmholtz pair driven by a precision current source. Fifteen volts were placed across the GMR bridge, and a 20 dB differential preamplifier was used to amplify the output voltage of the sensor. Measurements of the sensor output versus external field were made, and the results are displayed in Figure 3. First, note the output voltage increases with the magnitude of the external field, being insensitive to the field direction. The output appears to be quite linear with increasing field magnitude for fields above approximately 4 oersted, with considerable hysteresis observed in the low field measurements. This hysteresis is mainly due to the flux concentrator material, although slight hysteresis of the GMR elements themselves may contribute to the overall effect. The slope of the output voltage versus applied field gives the sensitivity of the sensor. As can

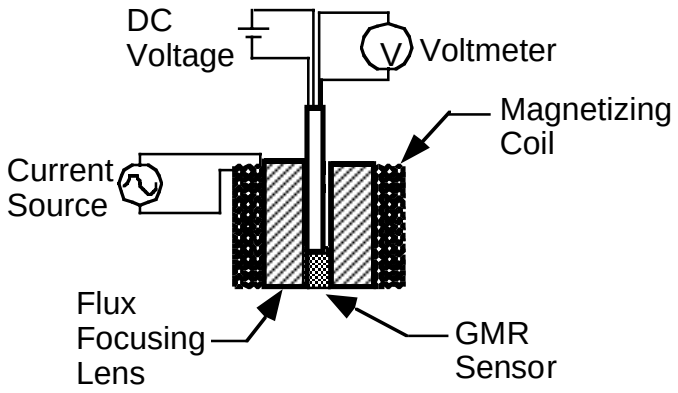

Figure 2. Schematic diagram of GMR based Self-Nulling Probe.

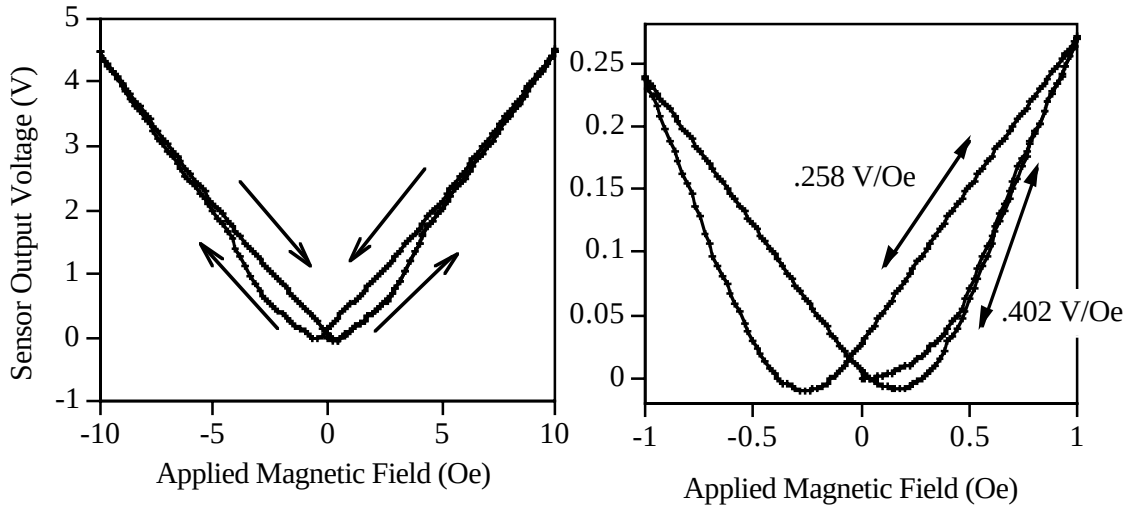

Figure 3. Calibration data for GMR sensor.

be seen in Figure 3, the slope at 0.5 oersted varies between approximately 258 mV/Oe and 402 mV/Oe due to the hysteresis of the sensor.

The GMR sensor was then installed into the Self-Nulling Probe and the output voltage examined. The oscilloscope traces for the voltage across the drive coil and the sensor output voltage are shown in Figure 4. The data were acquired using a 275 Hz drive with 15 volts across the GMR bridge and 20 dB preamplification. Note that the output signal is rectified due to the insensitivity of the GMR sensor to the direction of the applied field. To automate data acquisition and processing as well as improve the signal to noise ratio a lock-in amplifier tuned to the second harmonic of the drive signal was used. This corresponds to the main frequency component of the sensor output, as is evident from Figure 4. The data acquisition and processing scheme was therefore to monitor the output

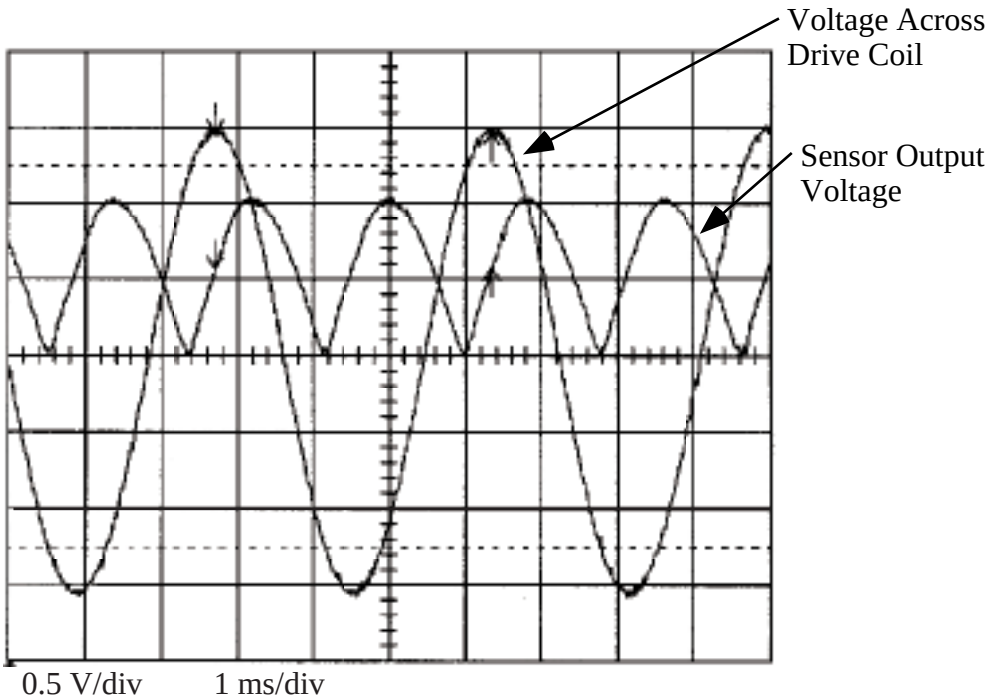

Figure 4. Drive and sensor waveforms for VLF Self-Nulling Probe.

amplitude of the GMR sensor at the frequency corresponding to the second harmonic of the drive signal. A finite element model of the VLF Self-Nulling Probe was constructed to investigate the field distribution of the probe. The effects of flaws in the material under test were also modeled. Figure 5 shows the axisymmetric finite element model and the flux lines for the probe operating at 200 Hz. In this model the material under test is a multi-layer stack of 0.1 cm thick aluminum alloy plates. It is clear from the figure that the magnetic field is reaching deeply into the material under test. It is also seen that the direct coupling between the drive coil and the sensor is reduced by the shielding effect of the flux-focusing lens.

FINITE ELEMENT MODELING RESULTS

In Figure 6 the magnetic field amplitude along the centerline of the probe is plotted for both an unflawed sample and a sample containing a flaw in the seventh layer of the 0.1 cm lay-up. This flaw was modeled by changing the material properties of the seventh layer from those of aluminum to air. Note that the peak field level along the probe centerline occurs within the material under test and that for z greater than approximately 0.5 cm the field level quickly diminishes to zero. This indicates that the lens is providing adequate shielding and focusing of the low frequency field for inspection deep into the material under test. Comparing the field level between the flawed and unflawed sample, the seventh layer flaw is seen to cause only a very small change in the amplitude at the probe face. The change in magnitude is 2.9 mOe above the unflawed level of approximately 0.5 Oe. Fortunately, this perturbation is within the measurement capabilities of the GMR sensor, as is seen in the calibration data shown in Figure 3.

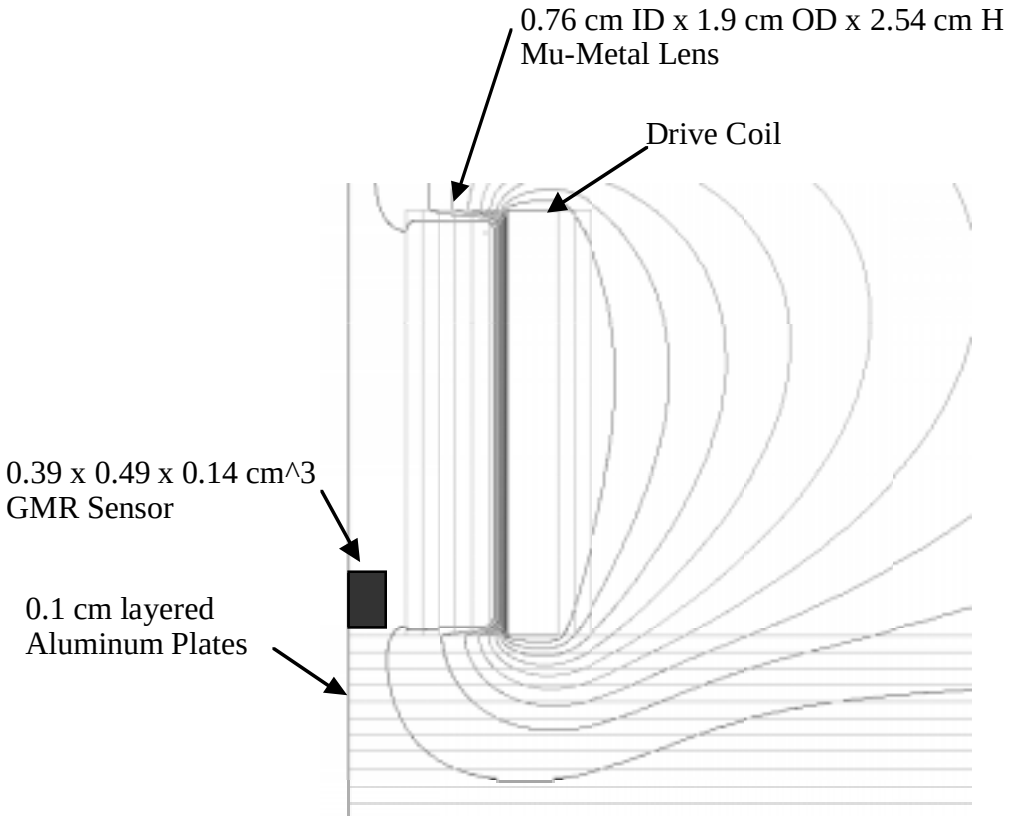

Figure 5. Finite element modeling results for the flux lines around the VLF Self-Nulling Probe operating at 200 Hz.

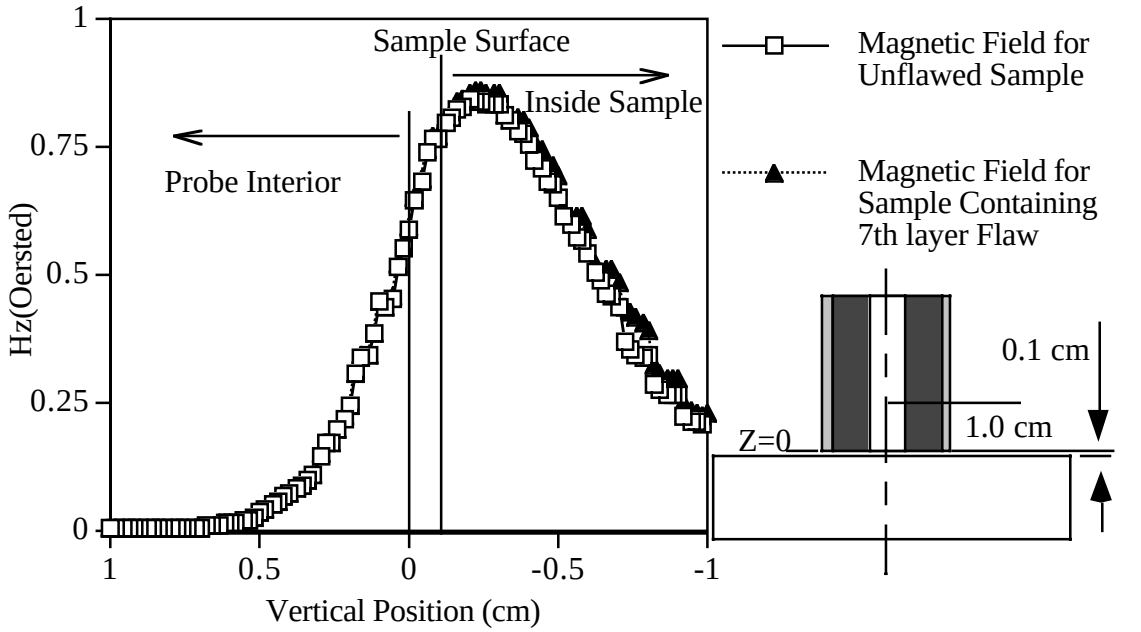

Figure 6. Finite element modeling results for the magnetic field along the probe centerline. Results are shown for unflawed sample and sample containing flaw in the seventh layer of 0.1 cm aluminum alloy lay-up.

EXPERIMENTAL RESULTS

The flaw detection capabilities of the VLF Self-Nulling Probe were examined on multi-layer aluminum alloy samples with actual fatigue cracks and fatigue cracks simulated by EDM notches. The first sample tested was a two layer aluminum alloy lay-up. The top layer was formed of an unflawed 4.76 mm thick plate. The lower layer was formed from a 1 mm thick aluminum plate with fatigue cracks grown from either side of a drilled center hole. The sample was scanned from the unflawed side with the probe operating at 1 kHz. The output of the GMR bridge was monitored with a lock-in amplifier referenced to the second harmonic of the drive signal, as explained previously. The RMS amplitude of the second harmonic component of the sensor output was recorded at each location of a raster scan over the flawed area. Figure 7 displays the sample geometry and C-scan results.

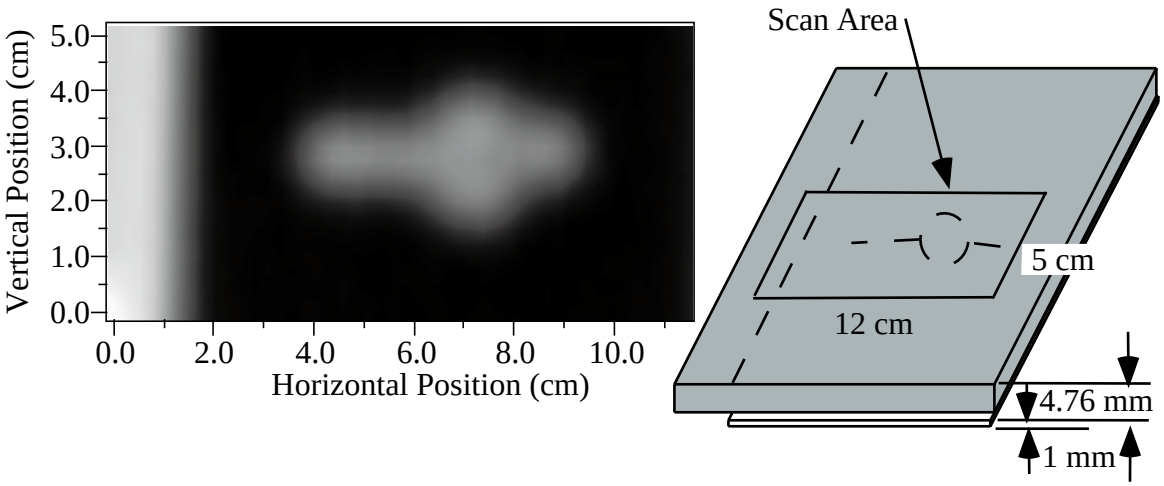

Figure 7. C-scan and sample geometry for detection of fatigue crack through 4.76 mm unflawed aluminum plate.

The second sample was designed to examine the flaw detection capabilities of the probe through varying thickness of unflawed material. A set of thirteen, 1 mm thick, aluminum plates with a cross section of 15 x 15 cm^2 was obtained. An EDM notch of 1.4 x 0.0127 cm^2 was placed in the center of one of the plates. The location of this flawed layer within the stack of unflawed plates was then varied, and data were acquired over the flawed area in each case. Figure 8 displays the C-scan results for the flawed plate placed in the 6^{th}, 7^{th}, 8^{th}, and 10^{th} layers. To maintain adequate depth of penetration of the magnetic field the operating frequency was lowered as the flaw depth increased. The plots in Figure 8 were acquired at a frequency of 600, 500, 400, and 135 Hz for the 6^{th}, 7^{th}, 8^{th}, and 10^{th} layer flaws respectively. The signal of the EDM notch is very clear in the 6^{th} and 7^{th} layer plots. For the 8^{th} layer the background noise is seen to approach the level of the flaw signals, although the notch signature is still evident in this as well as the 10^{th} layer plot. All of the data except the 10^{th} layer scan was recorded using a 40 dB preamplifier. The increased background level due to the 135 Hz operating frequency forced a reduction in preamplification to 20 dB. This increase in the overall probe output voltage with decreasing frequency is a result of an increase in flux leakage around the flux focusing lens which reduces probe sensitivity by decreasing the signal to noise ratio.

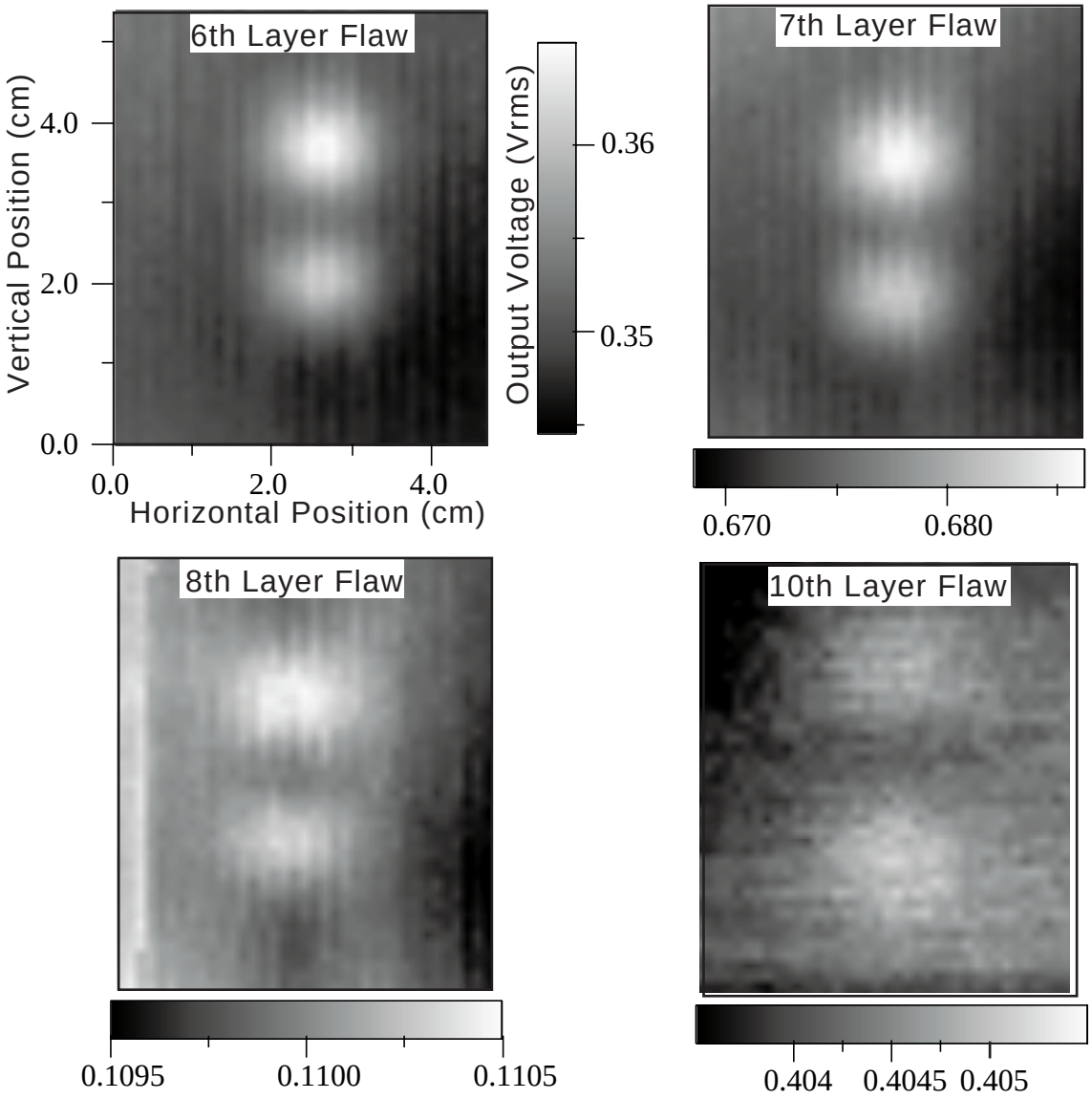

Figure 8. C-scan plots illustrating detection of EDM notch in thick, multi-layered conducting materials.

SUMMARY

It is clear from simple skin depth considerations that steady state electromagnetic inspection of thick multi-layered conductors requires low frequency excitation. Conventional pickup sensors, however, lose sensitivity at lower frequencies. Giant-magneto resistive materials offer a unique alternative for very low frequency electromagnetic NDE due to their high sensitivity to low frequency fields, small size, ease of use, and low cost. This paper outlines the development and testing of a Very Low Frequency Self-Nulling Probe incorporating a GMR sensor. The initial test results show flaw detectability at depths up to 1 cm in aluminum 2024. Optimization of the probe design based upon finite element modeling and GMR sensor characteristics (including hysteresis, linearity and saturation) is under way.

REFERENCES

1. J.D. Jackson, *Classical Electrodynamics*, pp. 210, 296-298, John Wiley &Sons, 1975.
2. H.L. Libby, *Introduction to Electromagnetic Nondestructive Test Methods*, John Wiley & Sons, 1971.
3. W. F. Arvin, *Review of Progress in QNDE*, Vol. 15, 1145, Plenum Press, New York, 1996.
4. E.S. Boltz and T.C. Tiernan, *Review of Progress in QNDE*, Vol. 17, 1033, Plenum Press, New York, 1998.
5. *NVE Sensor Engineering and Application Notes*, Nonvolatile Electronics, INC., 1997.
6. B. Wincheski, J.P. Fulton, S. Nath, M. Namkung, and J.W. Simpson, "Self-Nulling Eddy Current Probe for Surface and Subsurface Flaw Detection," *in Materials Evaluation*, Vol. 52/Number 1 (January 1994).